

Reduction of Optical Rotation and Scattering in a Cholesteric Liquid Crystal Layer

Mitsunori Saito and Junki Fujiwara

Department of Electronics and Informatics, Ryukoku University, Seta, Otsu 520-2194, Japan

Keywords: Liquid Crystal, Polarization, Optical Rotation, Scattering, Refractive Index.

Abstract: Cholesteric liquid crystal usually exhibits an optical rotation owing to its chirality. In the infrared region, however, the optical rotation power disappears, since the light wavelength is too long to recognize the refractive-index change of the nanometer-sized chiral structure. Consequently, the cholesteric liquid crystal exhibits a polarization-independent refractive index in the long-wavelength infrared range. The effective refractive index takes a value between the ordinary and extraordinary indices regardless of the polarization direction. The refractive index decreases to the ordinary index, when a phase transition takes place by application of an electric voltage (the electro-optical effect). This polarizer-free device operation, however, used to be limited to the wavelength range beyond 4 μm , since the optical rotation remained in the short wavelength range. In addition, a heavy scattering occurred during the phase transition process. In this study, experiments were conducted to examine how the chiral pitch and the thickness of the liquid crystal layer affected these optical characteristics. When a liquid crystal with a chiral pitch of 5 μm was enclosed in a cell with a 3 μm gap, both the rotation power and scattering loss were reduced successfully in a wide spectral range extending to 2 μm wavelength.

1 INTRODUCTION

Liquid crystals (LCs) are used widely in various technical fields today (Khoo, 2007). Although LCs exhibit efficient electro-optic effects, i.e., notable changes in the refractive index or optical rotation power by low-voltage application, they usually need a polarizer that halves a light intensity. This problem is serious in the infrared spectral range, in which efficient, durable, low-cost polarizers are unavailable due to opaqueness of ordinary glasses, crystals, and polymers (Saito and Yasuda, 2010). Since the early days of the LC device development, many researchers have conducted experiments to attain polarization-independent optical functions. A beam-splitting method (Patel and Maeda, 1991), for example, was used for creating a wavelength-division multiplexing device (Hirabayashi et al, 1993) and an infrared Lyot filter (Saito and Hayashi, 2013). A polarization-insensitive hologram was realized by use of a quarter-wave plate (Moore et al, 2008). A stack of orthogonally-oriented LC layers, which yielded an equivalent optical response for all polarization directions, was used for creating an optical phase

modulator (Lin et al, 2005) or a tunable lens (Ye et al, 2006). An axially-symmetric director distribution (Lee et al, 1999) and a complicated grating texture (Provenzano et al, 2006) were also constructed by coating special alignment films on the substrates.

Flat-panel displays use a twisted nematic LC, in which molecules take a chiral texture. As a light beam with a linear polarization propagates in this texture, its polarization direction rotates according to the director rotation (Saito et al, 2011). In a long-wavelength range, however, the optical rotation power decreases as the birefringence of the LC layer decreases (Patel and Lee, 1991). Generally, a material with a non-uniform structure exhibits uniform or isotropic optical properties, if the structure is smaller than the light wavelength (the effective medium theory). This is the case with the blue phase LC (Crooker, 2001), in which a nano-sized domain texture induces an isotropic refractive index (Haseba, 2005). Although this characteristic is useful for creating a polarization-independent optical device, the blue-phase LC has to be stabilized in a polymer matrix, and hence, needs a high voltage (~ 100 V) to induce an index change of $\Delta n=0.05$. (Lin et al, 2010).

A cholesteric (chiral nematic) LC is another selection to attain isotropic properties with a nano-sized structure of the molecular orientation (Hsiao et al, 2011). The chiral texture of the cholesteric LC is similar to that of the twisted nematic LC but possesses a shorter chiral pitch. The cholesteric LC, therefore, induces an optical rotation only for a light beam whose wavelength is sufficiently shorter than the chiral pitch. If the chiral pitch is close to the measurement wavelengths, a photonic band-gap emerges in the transmission spectrum (Kopp et al, 1998), which is useful to create a tunable laser (Furumi et al, 2003). In a longer wavelength range, however, the dimension of the molecular rotation is too small to be recognized by lightwave, and consequently, the cholesteric LC exhibits an isotropic index of refraction.

In a previous study, the authors examined infrared transmission characteristics of a cholesteric LC in order to realize a polarization-independent Fabry-Perot filter (Saito et al, 2015). An isotropic refractive

index was attained in the infrared range beyond $2 \mu\text{m}$ wavelength, and it decreased by 0.09 during a voltage application process (12–18 V). The transmitted light, however, exhibited a trace of optical rotation in the wavelength range below $3 \mu\text{m}$. In addition, the transmittance decreased heavily in the midway of the index change, which originated from the scattering in the unstable phase transition process (Kim et al, 2010). In this study, we conduct experiments to clarify how the chiral pitch and the LC layer thickness affect the transmission properties of the LC cell. On the basis of the experimental results, we discuss a suitable design of the LC cell to create a polarization-independent device with a reduced scattering loss.

2 PRINCIPLE

Figure 1 illustrates various LC phases in a cell together with polarization directions of propagating lightwave. As Fig. 1(a) shows, ordinary cells align

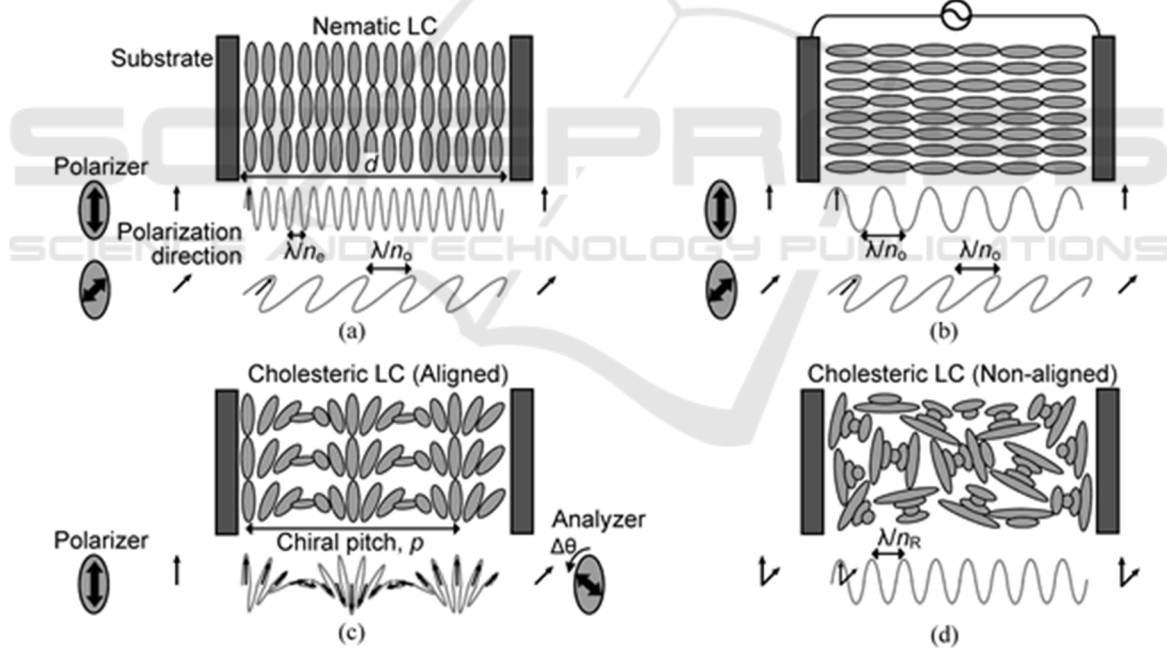


Figure 1: Various molecular orientations in a LC cell (thickness d). The refractive indices of the LC are n_o and n_e for the ordinary and extraordinary lightwaves (wavelength: λ), respectively. (a) A nematic LC that is oriented parallel to the substrate. The light wavelength in the LC cell is λ/n_e or λ/n_o depending on the polarization direction. (b) A homeotropic phase in which LC molecules are oriented in the direction perpendicular to the substrates owing to an electric field. The light wavelength in this LC cell is λ/n_o regardless of the polarization direction. (c) A cholesteric LC that is oriented by an alignment coating on the substrate surface. The director of the LC molecules rotates 360° with a chiral pitch, p . Accordingly, the polarization direction of a light beam rotates with the same pitch as it propagates in this LC. The polarization direction of the transmitted light can be analyzed by rotating an analyzer (polarizer) to find an angle $\Delta\theta$ that yields the maximum transmittance. (d) A cholesteric LC in a cell with no alignment coating. The LC layer consists of multiple domains in which molecules form a chiral structure. If the light wavelength is sufficiently long, this LC layer exhibits an effective refractive index, n_R , that is independent of the polarization direction. When an electric voltage is applied to the cells in (a), (c), and (d), they all turn to the homeotropic phase in (b).

nematic LC molecules in a fixed direction by the use of an alignment coating on the substrates. This LC orientation exhibits an ordinary or extraordinary refractive index, n_o or n_e , depending on the polarization direction of incident light. Consequently, a propagating beam takes a different wavelength, λ/n_o or λ/n_e , depending on the polarizer direction. As Fig. 1(b) shows, the LC molecules are reoriented in the direction of the electric field, if a voltage is applied between the substrates. In this phase, the LC exhibits an ordinary index (n_o) regardless of the polarization direction, and accordingly, the light wavelength becomes λ/n_o . In other words, only the extraordinary light suffers the change in the refractive index (wavelength). No index change takes place for the ordinary light. This is the reason that polarizers are needed for tuning LC devices.

Figure 1(c) is a schematic illustration of the cholesteric LC that is sandwiched between two substrates with an alignment coating. The LC director rotates 360° with a chiral pitch, p . A short-wavelength beam changes its polarization direction with the same pitch. Consequently, the polarization direction of the output beam becomes different from that of the input beam. The polarization state of the beam can be analyzed by rotating an analyzer (polarizer); i.e., if the polarization direction of the beam rotates by $\Delta\theta$ in the LC cell, the maximum transmittance is attained at the same angle, $\Delta\theta$. If the light wavelength is too long to recognize the chiral texture, the refractive index becomes independent of the polarization direction and takes an average of n_o and n_e . According to the effective medium theory (Born and Wolf, 1980), the average has to be taken for the dielectric constant, i.e., the square of the refractive index. The average index is therefore

$$n_{AV} = \sqrt{(n_o^2 + n_e^2)/2} . \quad (1)$$

This average index is higher than n_o , since n_e is usually higher than n_o . When a voltage is applied, the LC layer turns to the homeotropic phase in Fig. 1(b), and hence, the refractive index decreases to n_o .

The chiral texture of the cholesteric LC is affected seriously by the substrate surface. If the alignment coating on the substrate is removed, the regular arrangement of the LC molecules is disturbed heavily, and a domain texture emerges in the LC layer, as shown in Fig. 1(d). In this texture, the refractive index varies randomly in a small region, and consequently, isotropic properties are readily attainable in the long wavelength range. According to the effective medium theory above, the refractive index of this texture is

$$n_R = \sqrt{(2n_o^2 + n_e^2)/3} , \quad (2)$$

since one direction is parallel to the LC director (extraordinary light) and the other two directions are perpendicular to the director (ordinary light). A voltage application causes the LC molecules to turn to the electric field direction, and finally takes the homeotropic phase in Fig. 1(b). In this manner, the refractive index is adjustable between n_o and n_R independent of polarization. In the short wavelength range, however, the LC does not act as a uniform, isotropic medium, and hence the polarization state of the incident beam is not maintained. The optical scattering also increases as the wavelength becomes shorter. The scattering loss is notable particularly in the non-aligned cholesteric LC, since the molecular arrangement is disturbed heavily in this phase.

3 SAMPLES AND EXPERIMENTS

Samples were prepared by injecting a cholesteric LC into a gap between two silicon (Si) plates of 20 mm square (Saito et al, 2007). The gap or the LC layer thickness was adjusted between 3 and 20 μm by the use of glass spheres. No alignment coating was achieved on the substrate, since the polymer coating caused an absorption in the infrared region. The LC layer therefore took the domain texture shown in Fig. 1(d). The chiral pitch of the cholesteric LC (JNC Corporation, JD-1036LA, JD-1036LB) was $p=4.8$ or $1.5 \mu\text{m}$. The ordinary and extraordinary refractive indices were $n_o=1.52$ and $n_e=1.76$, respectively. According to Eq. (2), the effective index of the LC layer was assumed to be $n_R=1.60$. It was expected, therefore, that the index change of $\Delta n \approx 0.08$ was attainable by voltage application.

Electric wires were soldered on the substrates for voltage application. A sinusoidal signal of 1 kHz was generated by an electric oscillator and an amplifier. A peak voltage was adjusted between 0 and 100 V by monitoring the signal with an oscilloscope. The sample was mounted on the sample stage of a Fourier-transformation infrared spectrometer (FTIR, Shimadzu, IR Affinity-1) for spectral measurements. No polarizers was used in regular transmittance measurements. A polarization dependence of the transmittance was examined by inserting a BaF_2 wire-grid polarizer (Edmund, WGP8203) in front of the LC cell. As Fig. 1(c) shows, another polarizer (analyzer) was inserted on the output side, when the optical rotation was examined. In all measurements,

transmittance was evaluated by taking the ratio of transmitted light intensities that were measured before and after mounting the LC cell on the stage. The transmission characteristics of the polarizers were therefore cancelled out in the measured transmission spectra.

4 RESULTS

4.1 Conventional LC Cell

The first LC cell was prepared by using spheres of 20 μm diameter and the LC with a 4.8 μm pitch. The black lines in Figs. 2(a)–2(c) show the transmission spectra that were measured before and during a voltage application process. Interference peaks were visible over the entire spectral range. This interference was caused by the resonance in the LC layer (between the Si substrates), since the Si surfaces (the Si-LC boundaries) yielded a high reflectance owing to the high index of refraction. The high reflectance at the outer surfaces (the Si-air boundaries) reduced the maximum transmittance to $\sim 55\%$. The dips at 3.4 and 5.7 μm were attributed to the absorption by the LC. The spectral disturbance at 4.3 μm was caused by carbon dioxide gas that was contained in the atmosphere around the sample. The voltage application caused a transmittance decrease

(20 V) as well as the peak shift toward shorter wavelengths. When the voltage exceeded 20 V, the peak shift stopped. The transmittance returned to the original level at ~ 30 V, and thereafter no spectral change was visible.

The gray lines in Figs. 2(a)–2(c) indicate the peak wavelengths in the interference spectrum, which were calculated by assuming suitable values for the refractive index (n) and thickness (d) of the LC layer; i.e., according to the thin-film interference theory (Hecht, 1998), the peak wavelengths were calculated by the use of the relation,

$$\lambda_m = 2nd/m \quad (m = 1, 2, 3, \dots). \quad (3)$$

(The height and amplitude of these fitting curves have no meaning.) The peak-wavelength fitting was first conducted for the measured spectrum in Fig. 2(c), since the refractive index was presumed to be $n_o=1.52$ in the voltage application process [Fig. 1(b)]. By using this index value, the theoretical peak wavelengths were calculated for various thicknesses (d) to examine the coincidence of the measured and calculated peak wavelengths (the black and gray lines). The best fitting was attained when the thickness was assumed to be $d=20.1$ μm , which was close to the sphere (spacer) diameter. Then the peak fitting was conducted for the other spectra by using this thickness. The best-fit value was $n=1.52$ in Fig. 2(b) and 1.60 in Fig. 2(a). Figure 2(d) shows the

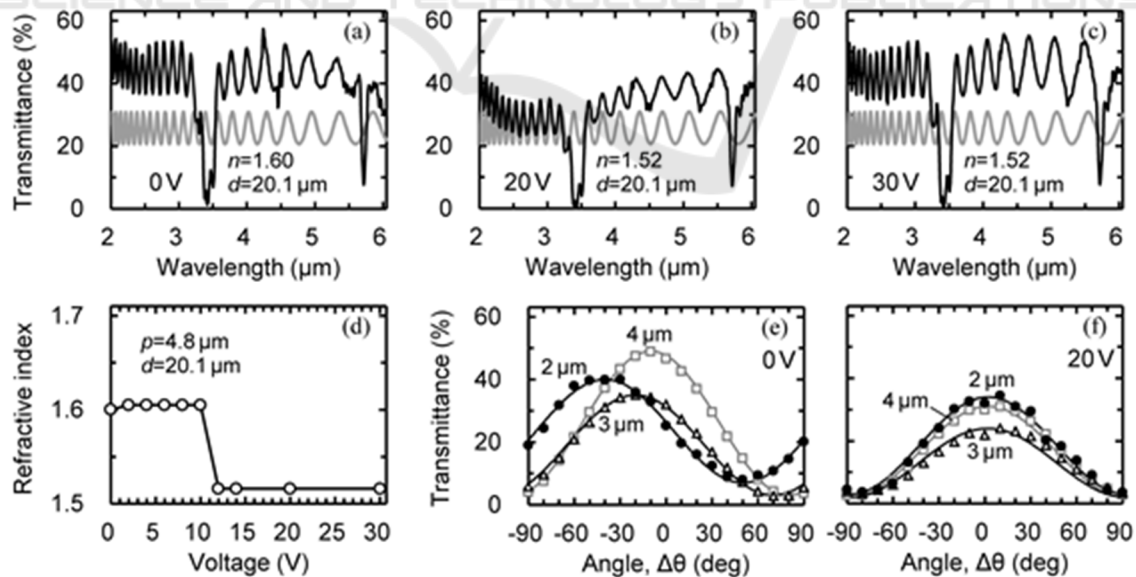


Figure 2: Optical properties of the LC with a chiral pitch of $p=4.8$ μm and an evaluated thickness of $d=20.1$ μm . (a–c) The black lines show the transmission spectra. The gray lines show the fitting curves that assume the refractive index of 1.52 at 30 V. (d) Evaluated refractive indices as a function of the applied voltage. (e, f) Transmittance change by the rotation ($\Delta\theta$) of the analyzer. Measurements were conducted at 0 and 20 V.

refractive indices that were evaluated in this manner. The refractive index decreases rapidly at around 10 V, and thereafter becomes constant. The transition to the homeotropic phase [Fig. 1(b)] takes place in this voltage range. A slight structural adjustment to complete the homeotropic orientation seems to continue until ~ 30 V, since the scattering remains even at a voltage exceeding 20 V. In the initial phase at 0 V, the evaluated refractive index is 1.60. This value is closer to $n_R=1.60$ than $n_{AV}=1.64$, which are calculated by using Eqs. (2) and (1), respectively, with $n_o=1.52$ and $n_e=1.76$. This fact confirms the assumption that the current LC initially takes the domain texture of Fig. 1(d).

The optical rotation in the LC cell was evaluated by using two polarizers, as shown in Fig. 1(c). Figures 2(e) and 2(f) show the transmittances that were measured as rotating the analyzer. During the voltage application process (20 V), the transmittance becomes the maximum at $\Delta\theta=0^\circ$ (parallel Nicols) and the minimum at $\pm 90^\circ$ (crossed Nicols). This result indicates that the light beam suffers no polarization rotation in this phase. In the initial phase at 0 V, however, the maximum angle shifts heavily at short wavelengths, indicating that the polarization direction rotates in the LC cell; e.g., 40° at $2 \mu\text{m}$ wavelength. As mentioned in Section 2, light with a short wavelength recognizes a fine index distribution, and consequently, the polarization direction rotates according to the molecular chirality.

4.2 LC with a Short Chiral Pitch

In the experiments above, the LC cell exhibited both the scattering loss and the optical rotation. These problems could be solved by using an LC with a short chiral pitch (a fine structure). An LC with a $1.5 \mu\text{m}$ pitch was therefore used to fabricate the next sample. The glass spheres of the same diameter ($20 \mu\text{m}$) were used as a spacer. The black lines in Figs. 3(a)–3(c) show the transmission spectra. Although the spectra were similar to those of the first sample, a high voltage was needed to induce the peak shift. A notable decrease in transmittance was also visible at around 60 V. The peak-wavelength fitting was conducted by drawing theoretical curves (gray lines) below the measured spectra. The LC layer thickness was evaluated to be $d=20.8 \mu\text{m}$ from the spectrum in Fig. 3(c). The evaluated indices were 1.60 at 60 V and 1.61 at 0 V. Figure 3(d) shows the refractive index as a function of the applied voltage. The refractive index of the initial phase (0 V) is 1.61, which is close to both the result of the first sample [Fig. 2(d)] and the predicted value (n_R) [Eq. (2)]. The refractive index decreases gradually to 1.58 as the voltage rises to 90 V, and then drops rapidly to 1.52. The cholesteric LC is a mixture of nematic and chiral LCs. Increase in the concentration of the chiral agent seems to raise a voltage that is needed to induce the reorientation.

Figure 3(e) shows the polarization state of the light beam that passed through the LC of the initial

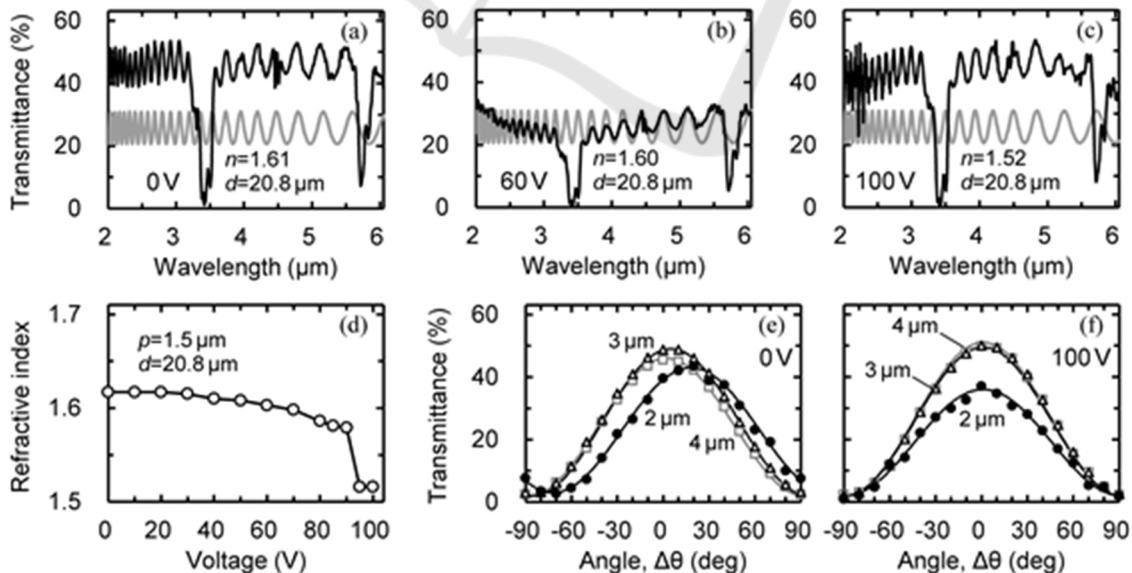


Figure 3: Optical properties of the LC with a chiral pitch of $p=1.5 \mu\text{m}$ and an evaluated thickness of $d=20.8 \mu\text{m}$. (a–c) The black lines show the transmission spectra. The gray lines show the fitting curves that assume the refractive index of 1.52 at 100 V. (d) Evaluated refractive indices as a function of the applied voltage. (e, f) Transmittance change by the rotation ($\Delta\theta$) of the analyzer. Measurements were conducted at 0 and 100 V.

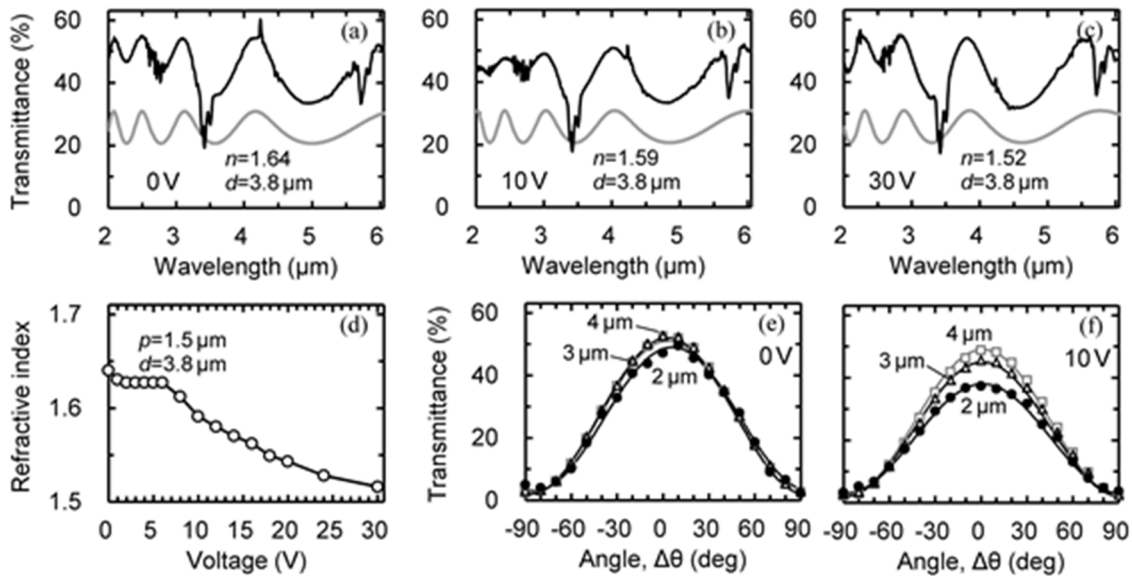


Figure 4: Optical properties of the LC with a chiral pitch of $p = 1.5 \mu\text{m}$ and an evaluated thickness of $d = 3.8 \mu\text{m}$. (a–c) The black lines show the transmission spectra. The gray lines show the fitting curves that assume the refractive index of 1.52 at 30 V. (d) Evaluated refractive indices as a function of the applied voltage. (e, f) Transmittance change by the rotation ($\Delta\theta$) of the analyzer. Measurements were conducted at 0 and 10 V.

phase. As expected, the optical rotation became smaller in comparison with the result in Fig. 2(e). At 2 μm wavelength, however, a slight rotation still remained. As Fig. 3(f) shows, no optical rotation occurred in the homeotropic phase at 100 V.

These results indicate that decreasing the chiral pitch neither eliminates the optical rotation and scattering nor reduces the operation voltage. We therefore reduced the LC layer thickness in the following experiment. Figures 4(a)–4(c) show the transmission spectra of the LC cell with a reduced thickness. The thickness was evaluated to be $d = 3.8 \mu\text{m}$ by fitting the theoretical curve to the spectrum in Fig. 4(c). In comparison with the spectra of the thick cells (Figs. 2 and 3), the spectral curve changes gently creating a smaller number of interference peaks. This happens because the peak interval extends as the optical thickness, nd , of the resonance cavity decreases [Eq. (3)]. The interference peaks shift to shorter wavelengths as the voltage increases. No notable transmittance decrease is visible during the voltage application process. Figure 4(d) shows the voltage dependence of the refractive index. The refractive index of the initial state (0 V) is 1.64. This index is higher than those of the former LC cells [Figs. 2(d) and 3(d)] and coincides with the theoretical value (n_{AV}) of Eq. (1). The LC seems to take a regular chiral texture [Fig. 1(c)] rather than a domain texture [Fig. 1(d)] when it is confined in a small volume. The

refractive index decreases gradually when the voltage rises exceeding 6 V.

Figure 4(e) shows the polarization state of the output beam. As regards a light beam of 3 μm wavelength or longer, no polarization rotation is visible. At 2 μm wavelength, however, a slight optical rotation still remains (10°). As Fig. 4(f) shows, the optical rotation becomes negligible when the LC is reoriented by the voltage application.

4.3 Reduction of the LC Thickness

As the experiments in the last section clarified, both the scattering loss and the optical rotation could be eliminated more effectively by decreasing the LC layer thickness than the chiral pitch. It was therefore assumed that the cholesteric LC of 4.8 μm pitch could also exhibit improved optical properties if it was confined in a thin cell. To confirm this assumption, we conducted experiments by using the long-pitch LC again.

The black lines in Figs. 5(a)–5(c) show the transmission spectra of the LC cell whose chiral pitch and thickness were $p = 4.8$ and $d = 7.2 \mu\text{m}$, respectively. The thickness was determined by the peak-wavelength fitting for the spectrum in Fig. 5(c). As Fig. 5(b) shows, this LC cell still exhibited a transmittance decrease during the phase transition process. The LC layer thickness was therefore

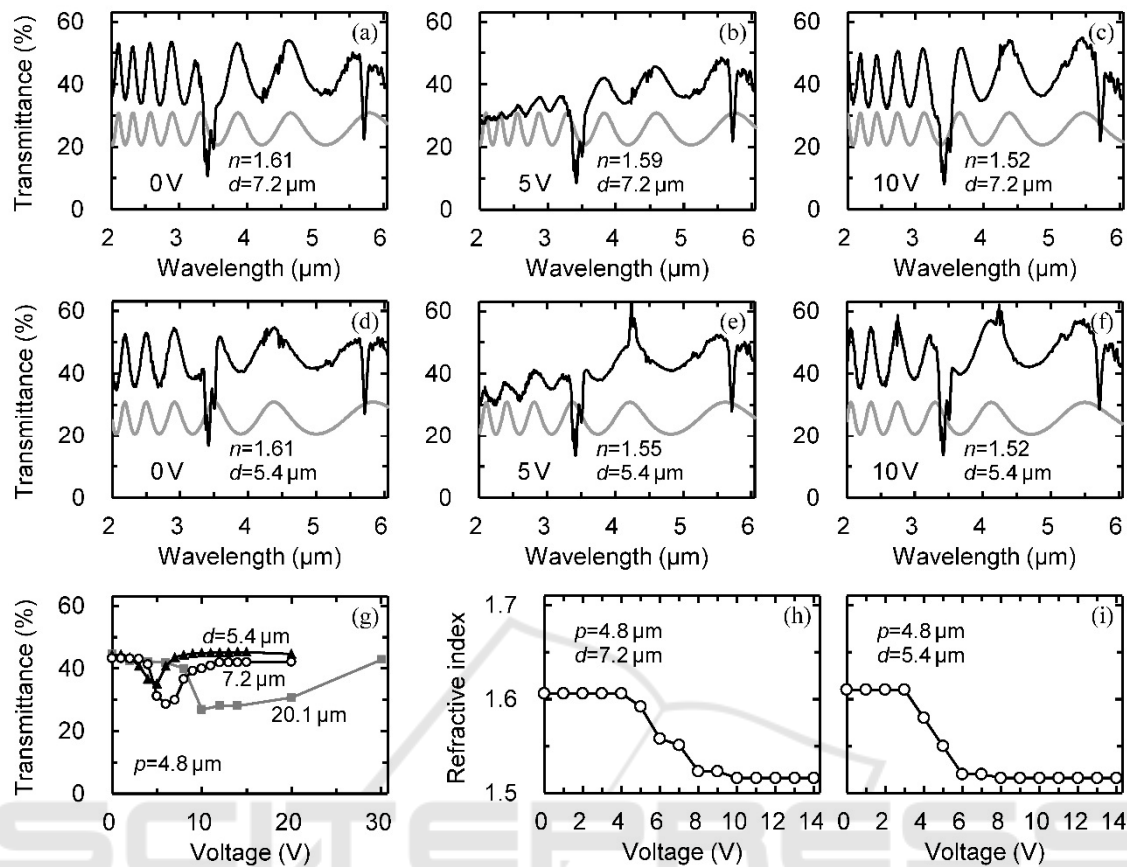


Figure 5: (a–f) Transmission spectra of the LC with a chiral pitch of $p=4.8 \mu\text{m}$ and an evaluated thickness of $d=7.2$ or $5.4 \mu\text{m}$. The black lines show the measured spectra. The gray lines show the fitting curves. The peak-wavelength fitting was conducted by assuming the refractive index of 1.52 at 10 V. (g) Average transmittance in the 2–3 μm range as a function of the applied voltage. The data were taken from the spectra that were exemplified in (a–f) and Fig. 2. (h, i) Evaluated refractive indices as a function of the applied voltage.

reduced further to $5.4 \mu\text{m}$. Figures 5(d)–5(f) show the transmission spectra of this LC cell. The thickness was still too large to reduce the scattering loss. Figure 5(g) shows voltage dependences of the transmittance, which were plotted by using the spectral data in Figs. 2(a)–2(c) and 5(a)–5(f). Since the transmittance changed heavily due to the interference, an average was taken over the 2–3 μm range. When the thickness was $20.1 \mu\text{m}$, the scattering occurred in the 8–30 V range. The scattering range decreased to 4–10 V in the $7.2 \mu\text{m}$ cell, and 3–6 V in the $5.4 \mu\text{m}$ cell. The scattering strength also decreased as the thickness decreased.

Figure 5(h) shows the refractive indices that were evaluated for the cell of $7.2 \mu\text{m}$ thickness. The refractive index in the initial phase (0 V) is close to the theoretical value, n_R [Eq. (2)]. The index decreases gradually in the 4–8 V range. This range coincides with the heavy-scattering range. As Fig.

5(i) shows, the LC cell of $5.4 \mu\text{m}$ thickness also exhibits a refractive index that is close to n_R . The index decreases to 1.52 in the 3–6 V range. In comparison with the thick LC cell [Fig. 2(d)], these thin cells exhibit a gentle index change with the increase of the applied voltage.

Finally, the LC cell of $2.9 \mu\text{m}$ thickness was prepared. Figures 6(a)–6(c) show the transmission spectra. The peak interval became large, since the optical thickness was small; i.e., $nd=4.7$ at 0 V and 4.4 at 10 V. As expected, no notable scattering was visible during the voltage application process. In addition, the absorption bands at 3.4 and 5.7 μm wavelengths became smaller owing to the reduction of the optical thickness.

Figures 6(d)–6(f) show the transmission spectra that were measured by using a linearly-polarized light beam. The probe beam of the spectrometer was polarized in the direction that was horizontal or

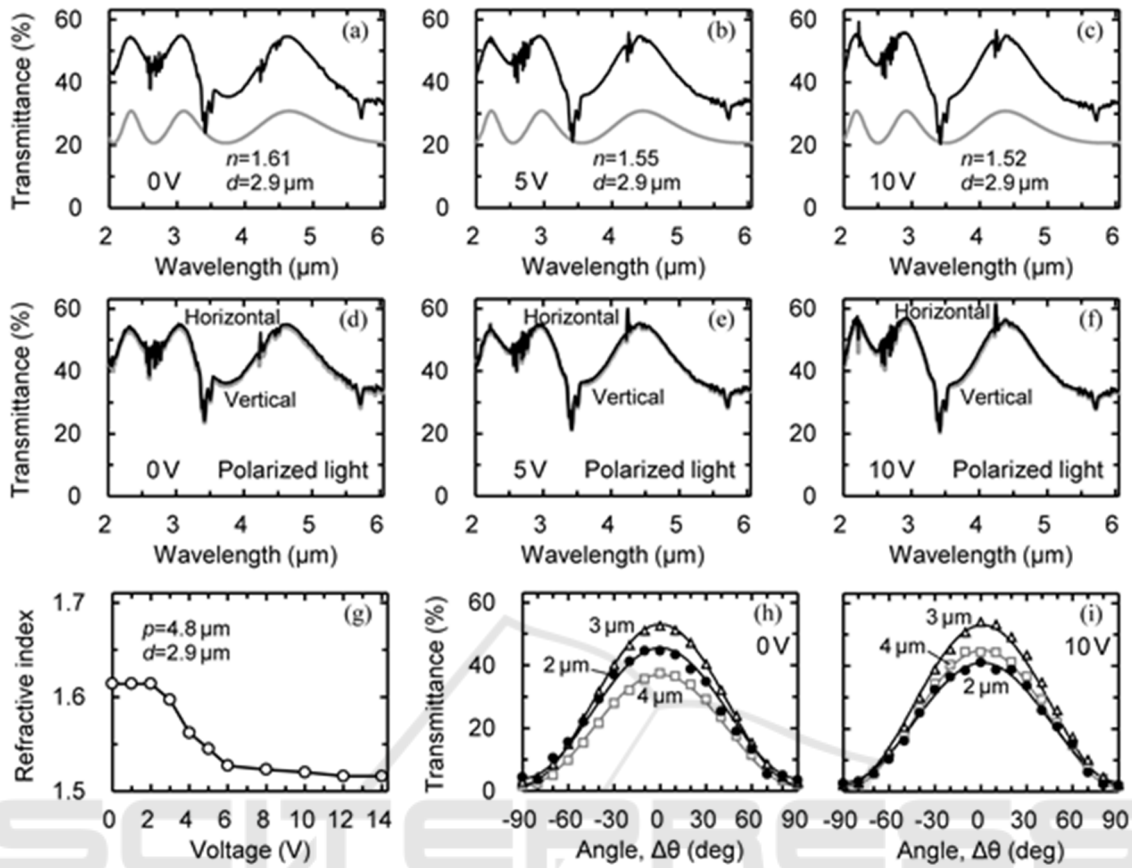


Figure 6: Optical properties of the LC with a chiral pitch of $p=4.8$ μm and an evaluated thickness of $d=2.9$ μm. (a–c) The black lines show the transmission spectra. The gray lines show the fitting curves that assume the refractive index of 1.52 at 10 V. Measurements were conducted by using non-polarized light. (d–f) The black and gray spectra (overlapping) were measured by using a probe beam that was linearly polarized in the horizontal or vertical direction. (g) Evaluated refractive indices as a function of the applied voltage. (h, i) Transmittance change by the rotation ($\Delta\theta$) of the analyzer. Measurements were conducted at 0 and 10 V.

vertical to the ground. As described in Section 3, the efficiency of the polarizer was cancelled out in the measured transmission spectra. The two spectra (the black and gray lines) corresponding to the horizontal and vertical polarizations overlap with one another in the entire spectral range. They also coincide with the spectra in Figs. 6(a)–6(c) that were measured with non-polarized light.

Figure 6(g) shows the refractive indices that were evaluated by the peak-wavelength fitting in Figs. 6(a)–6(c). The refractive index at 0 V was 1.61, which was close to the theoretical value, n_R . The index started to decrease at a lower voltage (2 V) in this cell than the former ones. It decreased slightly in the 6–12 V range, and thereafter became constant ($n_o=1.52$).

Figure 6(h) shows the polarization state of the beam that passed through the LC layer of the initial

phase. The transmittance took the maximum at $\Delta\theta=0^\circ$ and the minimum at $\pm 90^\circ$ even at 2 μm wavelength. That is, reduction of the optical rotation was successful in the entire spectral range. As Fig. 6(i) shows, the homeotropic phase at 10 V, of course, exhibited no trace of the optical rotation.

5 DISCUSSION

In our previous study, we evaluated the LC layer thickness or the cell gap (d) by using a transmission spectrum of the empty cell before injecting the LC. The cell gap, however, seemed to shrink during the LC injection process probably due to the surface tension. If this is the case, the inaccuracy of the thickness causes an error in the evaluation of the refractive index, since the peak-wavelength fitting

determines only the optical thickness (nd). The evaluation error becomes more serious as the thickness (gap) decreases. In this work, therefore, we evaluated the LC layer thickness from the spectrum of the reorientation state by assuming that the LC took the ordinary index ($n_o=1.52$) in this state [Fig. 1(b)]. This evaluation method seems successful, since evaluated indices are reproducible and plausible with reference to the theoretical prediction. The evaluated index change was $\Delta n=1.61-1.52=0.09$, and hence, the relative index change was $\Delta n/n_o=0.09/1.52=0.06$ (6%). Although this relative evaluation is accurate, the actual refractive index may be slightly lower than the evaluated value, since the ordinary index (n_o) is possibly lower than the assumed value ($n_o=1.52$ at $0.59\ \mu\text{m}$) because of the wavelength dispersion (Saito and Yasuda, 2003). Further analysis is needed to evaluate the refractive index more accurately.

The reduction of the LC layer thickness was effective to decrease the optical rotation, the scattering loss, the absorption loss (3.4 and $5.7\ \mu\text{m}$), and the operation voltage. This is an expected result, since these physical quantities change in proportion to the thickness. In addition to this proportional effect, a change in the microstructure (director distribution) seems to affect the optical properties, since both the surface tension and narrow space restrict the behavior of LC molecules.

6 CONCLUSIONS

A cholesteric LC with a chiral pitch of $4.8\ \mu\text{m}$ exhibited a polarization-independent refractive index in the infrared region ($>2\ \mu\text{m}$). The index change of $\Delta n=0.09$ was attainable by application of $10\ \text{V}$. Both the optical rotation and the scattering loss were eliminated successfully by enclosing this LC in a cell of $2.9\ \mu\text{m}$ thickness. This LC will be useful to create polarizer-free devices for the infrared optical systems.

REFERENCES

- Khoo, I. C., 2007. *Liquid Crystals*, Wiley, New York, 2nd edition.
- Saito, M., Yasuda, T., 2010. An infrared polarization switch consisting of silicon and liquid crystal. *J. Opt.* 12(1). p. 015504-1-6.
- Patel, J. S., Maeda, M. W., 1991. Tunable polarization diversity liquid-crystal wavelength filter. *IEEE Photon. Technol. Lett.* 3(8). p. 739-740.
- Hirabayashi, K., Tsuda, H., Kurokawa, T., 1993. Tunable liquid-crystal Fabry-Perot interferometer filter for wavelength-division multiplexing communication systems. *J. Lightwave Technol.* 11(12). p. 2033-2043.
- Saito, M., Hayashi, K., 2013. Integration of liquid crystal elements for creating an infrared Lyot filter. *Opt. Express*, 21(10). p. 11984-11993.
- Moore, J., Collings, N., Crossland, W. A., Davey, A. B., Evans, M., Jeziorska, A. M., Komarčević, M., Parker, R. J., Wilkinson, T. D., Xu, H., 2008. The silicon backplane design for an LCOS polarization-insensitive phase hologram SLM. *IEEE Photon. Technol. Lett.* 20(1). p. 60-62.
- Lin, Y.-H., Ren, H., Wu, Y.-H., Zhao, Y., Fang, Ge, J. Z., Wu, S.-T., 2005. Polarization-independent liquid crystal phase modulator using a thin polymer-separated double-layered structure. *Opt. Express*, 13(22). p. 8746-8752.
- Ye, M., Wang, B., Sato, S., 2006. Polarization-independent liquid crystal lens with four liquid crystal layers. *IEEE Photon. Technol. Lett.* 18(3). p. 505-507.
- Lee, J.-H., Kim, H.-R., Lee, S.-D., 1999. Polarization-insensitive wavelength selection in an axially symmetric liquid-crystal Fabry-Perot filter. *Appl. Phys. Lett.* 75(6). p. 859-861.
- Provenzano, C., Pagliusi, P., Cipparrone, G., 2006. Highly efficient liquid crystal based diffraction grating induced by polarization holograms at the aligning surfaces. *Appl. Phys. Lett.* 89(12). p. 121105-1-3.
- Saito, M., Yoshimura, K., Kanatani, K., 2011. Silicon-based liquid-crystal cell for self-branching of optical packets. *Opt. Lett.* 36(2). p. 208-210.
- Patel, J. S., Lee, S.-D., 1991. Electrically tunable and polarization insensitive Fabry-Perot étalon with a liquid-crystal film. *Appl. Phys. Lett.* 58(22). p. 2491-2493.
- Crooker, P. P., 2001. Blue Phases. Kitzerow, H., Bahr, C., eds., *Chirality in Liquid Crystals*. Springer, New York.
- Haseba, K., Kikuchi, H., Nagamura, T., Kajiyama, T., 2005. Large electro-optic Kerr effect in nanostructured chiral liquid-crystal composites over a wide temperature range. *Adv. Mater.* 17. p. 2311-2315.
- Lin, Y.-H., Chen, H.-S., Lin, H.-C., Tsou, Y. S., Hsu, H.-K., Li, W.-Y., 2010. Polarization-free and fast response microlens arrays using polymer-stabilized blue phase liquid crystals. *Appl. Phys. Lett.* 96(11). p. 113505-1-3.
- Hsiao, Y.-C., Tan, C.-Y., Lee, W., 2011. Fast-switching bistable cholesteric intensity modulator. *Opt. Express*, 19(10). p. 9744-9749.
- Kopp, V. I., Fan, B., Vithana, H. K. M., Genack, A. Z., 1998. Low-threshold lasing at the edge of a photonic stop band in cholesteric liquid crystals. *Opt. Lett.* 23(21). p. 1707-1709.
- Furumi, S., Yokoyama, S., Otomo, A., Mashiko, S., 2003. Electrical control of the structure and lasing in chiral photonic band-gap liquid crystals. *Appl. Phys. Lett.* 82(1). p. 16-18.
- Saito, M., Maruyama, A., Fujiwara, J., 2015. Polarization-independent refractive-index change of a cholesteric liquid crystal. *Opt. Mater. Express*, 5(7). p. 1588-1597.

- Kim, K.-H., Jin, H.-J., Park, K.-H., Lee, J.-H., Kim, J. C., Yoon, T.-H., 2010. Long-pitch cholesteric liquid crystal cell for switchable achromatic reflection. *Opt. Express*, 18(16), p. 16745–16750.
- Born, M., Wolf, E., 1980. *Principles of Optics*, Pergamon. Oxford. Chapter 2.
- Saito, M., Takeda, R., Yoshimura, K., Okamoto, R., Yamada, I., 2007. Self-controlled signal branch by the use of a nonlinear liquid crystal cell. *Appl. Phys. Lett.* 91(14), p. 141110-1–3.
- Hecht, E., 1998. *Optics*. Addison-Wesley. Reading, MA. Chapter 9.
- Saito, M. Yasuda, T., 2003. Complex refractive-index spectrum of liquid crystal in the infrared. *Appl. Opt.* 42(13), p. 2366–2371.

